THERMAL BEHAVIOUR OF STYRENE BUTADIENE RUBBER/POLY(ETHYLENE-CO-VINYL ACETATE) BLENDS
TG and DSC analysis

C. K. Radhakrishnan[1], *A. Sujith*[1] *and G. Unnikrishnan*[2*]

[1]Mohammed Abdurahiman Memorial Orphanage College, Manassery, Mokkam, Calicut 673602, Kerala, India
[2]National Institute of Technology, Calicut 673601, Kerala, India

The thermal behaviour of styrene butadiene rubber (SBR)/poly (ethylene-co-vinyl acetate) (EVA) blends was studied by using thermogravimetry (TG) and differential scanning calorimetry (DSC). The effects of blend ratio, cross-linking systems and compatibilization on the thermal stability and phase transition of the blends were analyzed. It was found that the mass loss of the blends at any temperature was lower than that of the components, highlighting the advantage of blending SBR and EVA. The addition of compatibilizer was also found to improve the thermal stability. DSC studies indicated the thermodynamic immiscibility of SBR/EVA system even in the presence of the compatibilizer. This is evident from the presence of two different glass transition temperatures, corresponding to SBR and EVA phases in both compatibilized and uncompatibilized blends.

Introduction

Thermal analysis is becoming an increasingly useful tool in material characterization. To develop durable industrial products from polymers, it is necessary to investigate the thermal stability of the basic matrices. Thermogravimetric analysis (TG) has proved itself as a successful technique in determining the thermal stability of polymers and polymer blends. A deep knowledge of the degradation and decomposition behaviour of macromolecules on heating is essential when these materials are processed and fabricated. The threshold temperatures for break down determine the upper limit of temperature in fabrication [1]. Differential scanning calorimetry (DSC) is another method where the heat flow rate associated with a thermal event is measured as a function of time and temperature, allowing us to obtain quantitative information about the melting and phase transitions. DSC analysis can also be used as an effective tool for evaluating the compatibility in polymer blends [2, 3].

Excellent reports on the thermal stability studies on polymers and their blends exist in literature [4–7]. Thavamani and Khastgir [8] reported the TG of poly(ethylene-co-vinyl acetate) (EVA) and hydrogenated nitrile rubber (HNBR) blends. The results showed that the thermal stability of EVA is improved upon blending with HNBR. Schmidt *et al.* [9] studied the thermal stability of blends of polyaniline and ethylene propylene diene rubber (EPDM), by TG. The results showed more than one stages of degradation and an improvement in the activation energy of degra-

dation upon blending. The thermal degradation behaviour of blends has been used to identify styrene butadiene rubber (SBR)/polybutadiene rubber (BR) blends from SBR based compounds by Amraee *et al.* [10] from the ratio of peak heights of DTG peaks. Ahmed *et al.* [11] compared the thermal stability of sulphur, peroxide and radiation cured NBR/SBR vulcanizates, using TG. They reported that the radiation cured formulation exhibited better thermal stability, compared to the other systems.

Sarkar *et al.* [12] evaluated the degradation behaviour of hydrogenated styrene butadiene rubber (HSBR) at high temperatures using TG and DSC. They found that the thermal stability of HSBR is higher compared to SBR. Ghosh *et al.* [13] investigated the thermal and oxidative degradation of polyethylene (PE)/EPDM rubber blends, vulcanized using sulphur accelerator system, by DSC and TG. The results indicated that sulphur vulcanization made the PE/EPDM blends thermally more stable. Rocco *et al.* [14] used DSC and optical microscopy to determine the miscibility and crystallinity of the blends of poly(ethylene oxide) (PEO) with poly(4-vinylphenol-co-2-hydroxyethyl methacrylate) (PVPh-HEM). A single glass transition temperature (T_g) was observed for all the blends, indicating miscibility. Lai and Liu [15] investigated the thermal properties of poly(ether-sulfone) (PES) and poly(phenylene sulfide) (PPS) with various compositions. The blends showed two glass transition temperatures corresponding to PPS-rich and PES-rich phases. Both the T_gs decreased obviously for

the blends with PES matrix. On the other hand, T_gs of PPS and PES phases decreased a little when PPS was the continuous phase.

SBR is a general purpose synthetic rubber having high filler-loading capacity, good flex resistance, crack-initiation resistance, and abrasion resistance. However, like other unsaturated rubbers, its ageing resistance is poor, due to the unsaturation in the butadiene component. In order to minimize the oxidative degradation of SBR during service at high temperature, it is advisable to blend it with a saturated or low unsaturated polymer. EVA copolymer may be considered as a good partner for this purpose because of its excellent ageing resistance, weather resistance, and mechanical properties. In addition, it can provide easier melt processability to the corresponding blends.

The curing behaviour, morphology, mechanical properties, swelling behaviour and ageing characteristics of SBR/EVA blends have been reported by our group earlier [16–18]. These blends were found to be immiscible with low interfacial adhesion between the components. The goal of the present work is to study the effects of blend composition, cross-linking systems and a compatibilizer (SEBS-g-MA) on the degradation behaviour, thermal stability, melting and the phase transition of SBR/EVA blends by using TG and DSC.

Experimental

Materials

SBR marketed under the trade name Syanaprene (SBR-1502) was obtained from Korea Kumho Petrochemical Co., Ltd. (Ulsan, Korea). EVA used was EVA-1802 obtained from National Organic and Chemical Industries Ltd. Mumbai, India. The basic characteristics of SBR and EVA are given in Table 1. The compatibilizer used was maleic-anhydride grafted poly[styrene-b-(ethylene-co-butylene)-b-styrene] (SEBS-g-MA) triblock copolymer, Kraton FG1901X, supplied by Shell Chemicals, Houston, Texas, USA,

having 29% styrene and 1.84% grafted maleic anhydride. The rubber chemicals used such as sulphur, dicumyl peroxide, zinc oxide, stearic acid and mercapto benzothiazyl disulphide (MBTS) were of commercial grade.

Blend preparation

The blends of SBR and EVA were prepared, on a laboratory type (150×300 mm) two roll mixing mill having a friction ratio of 1:1.4, as per ASTM D-15-627. The temperature of the rollers of the mill was kept at 30°C by the circulation of cold water. The different cross-linking systems used viz. sulphur (S), dicumyl peroxide (DCP) and mixed (S+DCP) have been indicated as S, P and M, respectively. The compounds having sulphur system are designated as S_0 (pure SBR), S_{20} (80/20 SBR/EVA), S_{40} (60/40 SBR/EVA) and so on. Similarly, the compounds with peroxide and mixed curing systems are designated respectively as P_0 and M_0 (pure SBR), P_{20} and M_{20} (80/20 SBR/EVA), P_{40} and M_{40} (60/40 SBR/EVA) and so on. The subscripts indicate the mass% of EVA in the blends. S_{100} and M_{100} samples could not be moulded, probably due to the saturated backbone of EVA. The compatibilizer, SEBS-g-MA used in this study, has been coded as C. The compatibilizer loading has been indicated by a subscript. For instance $P_{60}C_6$ indicates peroxide cured 40/60 SBR/EVA blend containing 6 phr of the compatibilizer and $S_{60}C_6$ indicates sulphur cured 40/60 SBR/EVA blend containing 6 phr of the compatibilizer. The compounding recipes of the blends are given in Table 2. The compounded blends were compression moulded at 160°C under a pressure of 6.7 MPa, for the optimum cure.

Methods

Thermogravimetry (TG)

TG and DTG were carried out using an instrument, TGA Q50 V2.34 Build 127. Samples were scanned from 30 to 800°C with a heating rate of 20°C min^{-1}.

Table 1 Details of materials

Materials	Characteristics		Source
Styrene butadiene rubber (SBR-1502)	styrene content/%	24.000	Korea Kumho, Petrochemicals Co. Ltd., Korea
	volatile matter/%	0.750	
	organic acid/%	4.750	
	soap/%	0.500	
	ash/%	1.500	
	antioxidant/%	0.500	
	density/kg m^{-3}	940.000	
	Mooney viscosity (ML$_{1+4}$; 100°C)	46.000	
Poly(ethylene-co-vinyl acetate) (EVA-1802)	melt flow index/kg/10 min	0.002	National Organic and Chemical Industries Ltd., Mumbai, India
	density/kg m^{-3}	940.000	
	Vicat softening point/°C	59.000	
	vinyl acetate/%	18.000	
	intrinsic viscosity/dL g	0.170	

Table 2 Formulation of the mixes (phr)

Ingredients/phr	Sulphur system	Peroxide system	Mixed system
Polymer	100	100	100
Zinc oxide	4	–	4
Stearic acid	2	–	2
*MBTS	1.5	–	1.5
Sulphur	2	–	2
Dicumyl peroxide	–	4	4

*mercaptobenzothiazyl disulphide

Differential scanning calorimetry (DSC)

DSC examinations of the blends were carried out using an instrument, DSC Q100 V 3.5 Build 175. The samples were inserted into the apparatus at room temperature and heated immediately to 200°C at a rate of 40°C min^{-1} and kept for one min at this temperature in order to remove the volatile impurities. They were then quenched to –80°C and the DSC scan was taken from –80 to 120°C at a heating rate of 5°C min^{-1} in helium atmosphere. The glass transition temperature (T_g) of each sample was taken as the mid point of transition in the DSC trace. The peak value of DSC curves was considered as the melting point. The area of the melting endotherm was calculated and has been reported as the heat of fusion. The fractional crystallinity (X_C) of the blends was calculated from the ΔH values.

Results and discussion

### Thermogravimetry

Effect of blend composition

The thermogravimetric plot of peroxide cured SBR is given in Fig. 1. The degradation starts at about 246°C and is completed at 503°C. The mass loss observed during this stage of decomposition is 98.05%. A residue of about 0.9% remains at 550°C. The mass loss observed at 350°C is 6.85% and that at 450°C
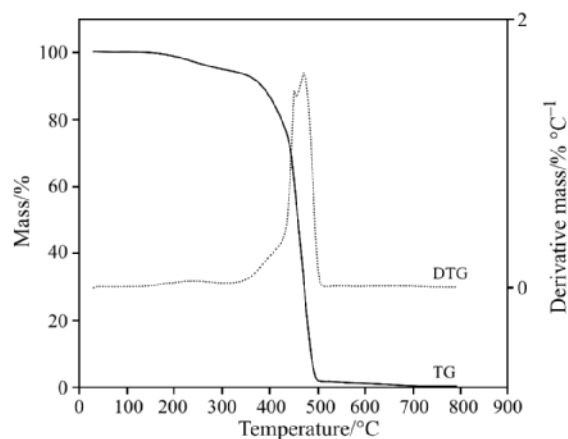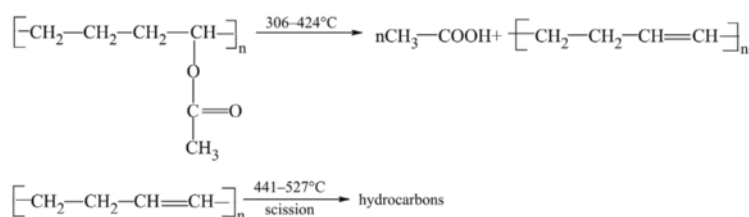

Fig. 1 TG and DTG curves of peroxide cured SBR

is 37.87%. In the DTG curve, the peak is observed at 474°C, which corresponds to the degradation of saturated and unsaturated carbon chains in SBR. This results in the formation of volatile monomer along with some amount of impurities. The mechanism of random scission of the polymer chains that can occur at high temperature is shown in Scheme 1.

The thermal decomposition of peroxide cured EVA is presented in Fig. 2. Two regions of degradation are observed. The first step of degradation starts at 306°C and is completed at 424°C. The second stage of degradation occurs in the region of 441–527°C. The former stage of degradation is due to the elimination of acetic acid from the vinyl acetate part of the chain and the later stage is due to the scission of polyene left after deacetylation [1]. The possible mechanism of the degradation process that occurs in EVA is shown in Scheme 2.

The mass loss observed during the first and second stages are 15.56 and 82.66%, respectively. About 1.3% remains as residue at 550°C. The mass loss observed at 350°C is 6.1% and that at 450°C is 33.64%. In the DTG curve the major peak is observed at 466°C, which corresponds to the scission of conjugated polyene left after deacetylation. A small peak corresponding to the deacetylation and degradation of polyethylene is observed at 368°C.
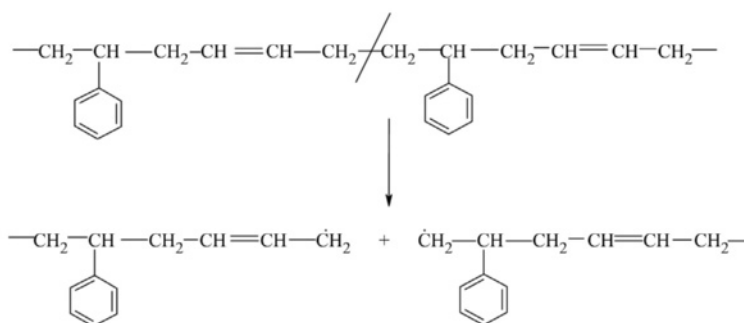
Scheme 1 Degradation mechanism of SBR
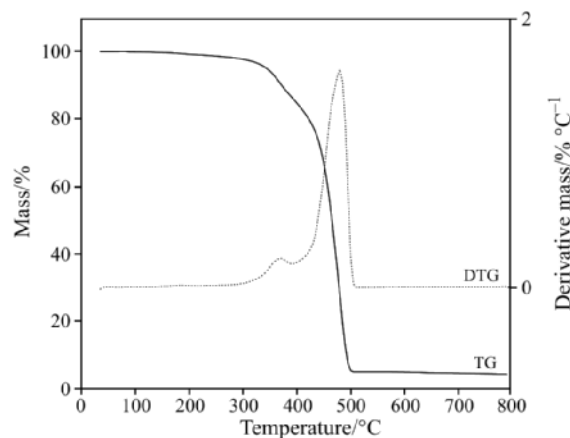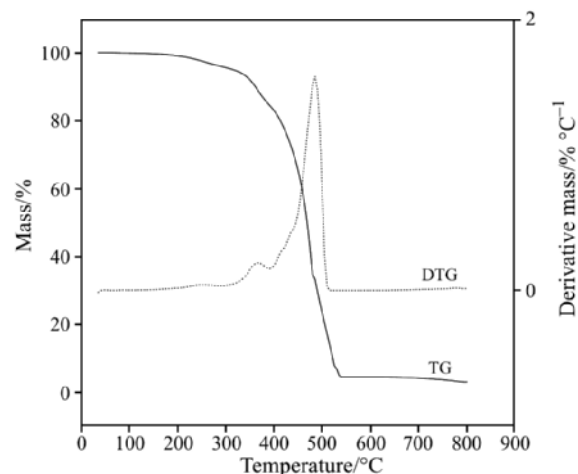
Scheme 2 Degradation of EVA

Fig. 2 TG and DTG curves of peroxide cured EVA

Fig. 3 TG and DTG curves of P_{60}

The degradation behaviour of the blends in general is marginally different from that of the individual components. It has been reported that the thermal stability of one type of polymer can be improved by the incorporation of a second polymer [19]. The thermogravimetric plot of peroxide cured 40/60 SBR/EVA blend is presented in Fig. 3. It can be observed that degradation occurs in two stages. The first and second stages of degradation occur in the region 266–418 and 432–545°C, respectively. The mass loss observed during the first and second stages of decomposition are 12.30 and 86.08%, respectively. About 1.54% remains as residue at 550°C. The mass loss observed at 350°C is 4.76% and that at 450°C is 29.47%. DTG curve indicates two peaks.

The first peak is around 370°C and the second peak around 484°C is a merged one for SBR and EVA.

The initial and final decomposition temperature and the mass loss at different temperatures of the different blends are given in Table 3. It may be noted that as the EVA content in the blend increases, the initial and final decomposition temperature are marginally enhanced. The initial decomposition temperature (T_0) and the temperature of 50% decomposition (T_{50}) are plotted as a function of blend composition in Fig. 4. Both T_0 and T_{50} show an increase with EVA content up to 60% of EVA. This is probably due to the enhanced interfacial adhesion between the

Table 3 Decomposition temperature and mass loss of different SBR/EVA blends

| Sample code	Decomposition temperature/°C		Mass loss/% at			Residue/mass% at
	initial	final	350°C	450°C	500°C	550°C
P_0	246	503	6.85	37.87	98.03	0.90
P_{20}	248	505	6.62	36.40	98.00	0.95
P_{40}	261	526	6.15	33.52	97.90	1.20
P_{60}	266	545	4.76	29.47	96.30	1.54
P_{80}	264	539	5.81	30.10	97.80	1.42
P_{100}	306	527	6.10	33.64	96.70	1.30
S_{60}	255	540	5.57	32.85	94.84	4.87
M_{60}	264	543	7.90	34.62	93.02	5.34
$P_{60}C_6$	269	549	4.35	29.10	94.26	2.68
$S_{60}C_6$	261	543	4.52	29.27	94.40	4.98
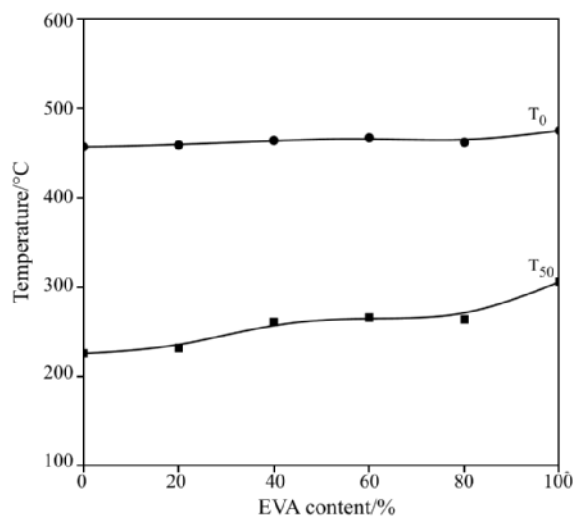
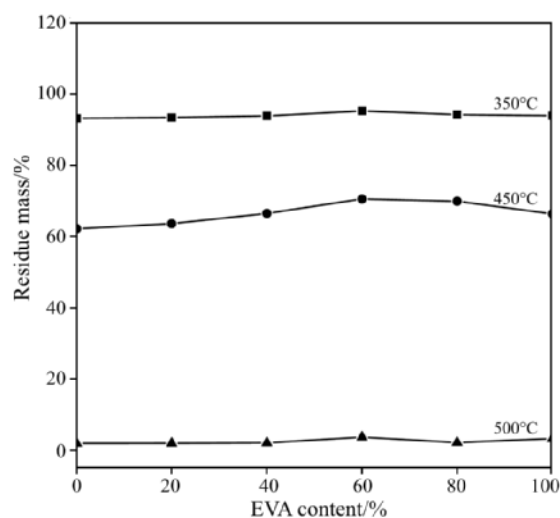**Fig. 4** Variation of T_0 and T_{50} of peroxide cured SBR/EVA blends

Fig. 5 Variation in residue mass of peroxide cured SBR/EVA blends

blend components. In Fig. 5 residue mass at different temperature is plotted as a function of blend composition. A slight increase in the residue mass is observed with the increase in the mass% of EVA up to 60% in the blends at 350, 450 and 500°C.

Effect of cross-linking systems

Initial decomposition temperature of 40/60 SBR/EVA blend systems cross-linked with sulphur, DCP and a mixed system are 255, 266 and 264°C, respectively. The DCP cured system show the highest initial decomposition temperature indicating its good thermal stability. This can be attributed to the nature and distribution of cross-links between the macromolecular chains of the blends as shown in Fig. 6. Sulphur vulcanization introduces mono-, di- and polysuphidic linkages between the macromolecular chains. The DCP vulca-
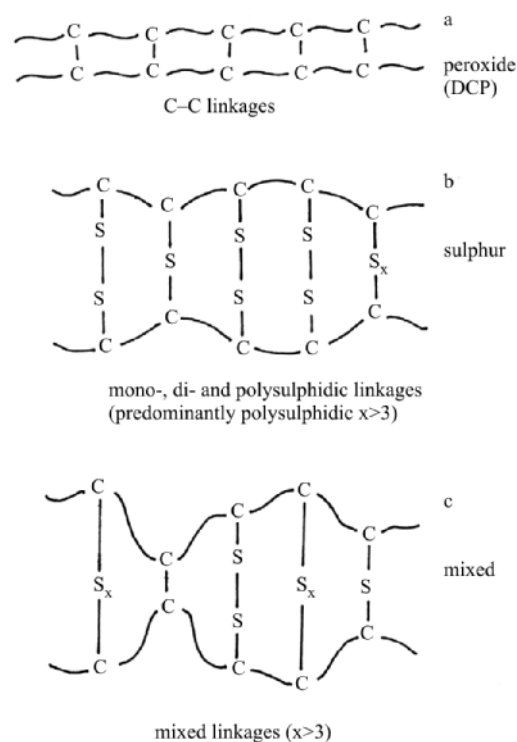

Fig. 6 Schematic representations showing the nature of cross-links formed by different cross-linking systems

nized system has only C–C rigid linkages and the mixed system contain both polysulphidic and rigid C–C linkages. The values of bond length and bond energy given in Table 4 also support this view. The C–C cross-links in the peroxide cured system are less flexible with the highest bond energy (355 kJ mol^{-1}). TG and DTG curves of S_{60} and M_{60} are given in Figs 7 and 8. All the DTG curves show two peaks i.e., at (364, 480°C), (370, 484°C) and (367, 483°C) for sulphur, peroxide and mixed systems, respectively. The mass loss observed at 350 and 450°C are given in Table 3. In these cases also, the peroxide cured system shows the lowest mass loss at a particular temperature.

Table 4 Bond length and bond energies of different types of chemical linkages

Type of bond	Bond length/nm	Bond energy/kJ mol^{-1}
C–C	0.154	355
C–S	0.181	267
S–S	0.188	238

Effect of compatibilizer

The results of the thermogravimetric analysis of peroxide and sulphur cured 40/60 SBR/EVA blends compatibilized with 6 phr SEBS-g-MA are presented in Table 3. There is an enhancement in the initial as well as final decomposition temperature upon compatibiliza-
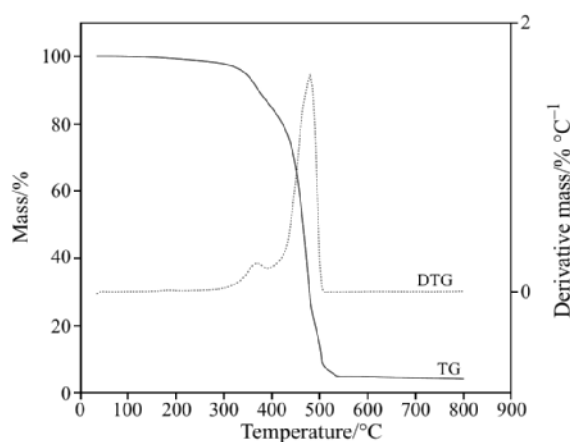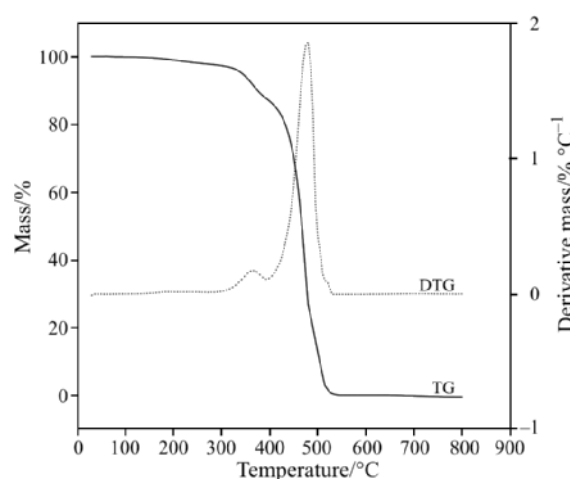
Fig. 7 TG and DTG curve of S_{60}

Fig. 8 TG and DTG curve of M_{60}

tion. DTG curves of compatibilized systems exhibit two peaks, a minor one around 371 and 368°C and a major one around 487 and 482°C, respectively, for peroxide and sulphur cured 40/60 SBR/EVA blends. From Table 3, it can be seen that the mass loss at 350, 450 and 500°C are lower for the compatibilized system compared to the uncompatibilized one. This indicates the improvement in the thermal stability of the system upon compatibilization.

Activation energy of degradation

The activation energy for the degradation process (temperature range 350–500°C) was calculated from the Arrhenius relationship,

$$X=X_0\exp(-E/RT) \qquad (1)$$

where X is the mass loss at a particular temperature, X_0 a constant, E the activation energy, R the universal gas constant and T the absolute temperature. The activation energy for the degradation process of all the systems is given in Table 5. It can be seen that the blends exhibited higher activation energy than the

Table 5 Activation energy for the degradation of SBR/EVA systems

Sample code	Activation energy, E/kJ mol^{-1}
P_0	10.88
P_{20}	10.98
P_{40}	11.21
P_{60}	12.16
P_{80}	11.33
P_{100}	11.22
S_{60}	11.53
M_{60}	9.95
$P_{60}C_6$	12.68
$S_{60}C_6$	12.35

pure components indicating the thermal stability achieved by blending. Among the various cross-linking systems, the peroxide cured system shows the highest activation energy for the process. This is due to the nature of cross-links introduced during vulcanization (Fig. 6) and their respective bond length and bond energy as explained earlier. In the mixed cured system, both types of linkages are present and its activation energy is closer to that of the sulphur cured system. Compatibilization also results in an increase in activation energy.

Differential scanning calorimetry (DSC)

The thermal properties of SBR, EVA, uncross-linked and cross-linked SBR/EVA blends were analyzed by using DSC. The DSC results of SBR, EVA and un-cross-linked 40/60 SBR/EVA blends are presented in Fig. 9. The peak point temperature is taken as the melting point (T_m) and the mid point of transition as the glass transition temperature (T_g). The area of the melting endotherm has been used to find the heat of fusion (ΔH). The percentage of crystallinity for EVA, with 18% vinyl acetate is 32, according to [20]. The observed ΔH value of EVA in the pure form is 42.2 J mol^{-1}. Percentage crystallinity of the blends was calculated using the observed values of ΔH. The melting temperature (T_m), heat of fusion (ΔH), fractional crystallinity (X_C) and the glass transition temperature (T_g) of the uncross-linked and cross-linked blends are reported in Table 6. It is observed that the fractional crystallinity and the heat of fusion values decrease with increase in SBR content. Martuscelli [21] showed that crystallinity was affected by blend composition and crystallisation conditions such as temperature, pressure, orientation, molecular mass and diluents. The crystallisation of polyethylene segment in EVA is controlled by the segmental diffusion rate of other polymeric chains. The separation is en-
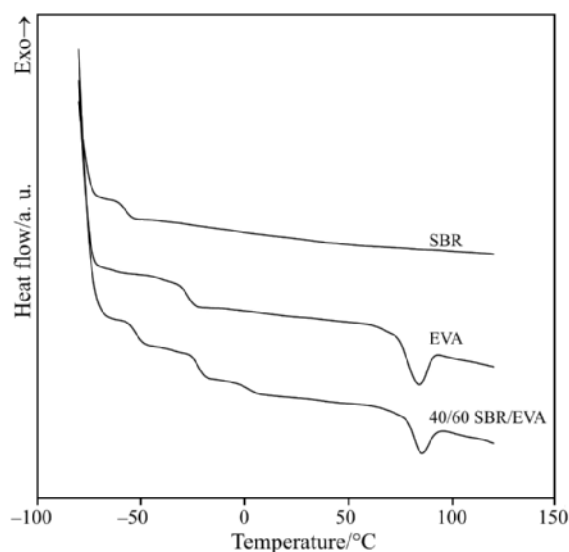
Fig. 9 DSC curves of uncross-linked SBR, 40/60 SBR/EVA and EVA

Fig. 10 DSC curves of P_0, P_{60} and P_{100}

hanced as the SBR content is increased. Incomplete crystallisation thus leads to a decrease in ΔH and crystallinity. It is interesting to note that the T_g values of SBR and EVA phases in uncross-linked blends do not undergo substantial shift. These observations coupled with the relatively insignificant increase in the T_m, with the incorporation of EVA, indicate the immiscibility of the blend system.

DSC results of peroxide cured SBR, EVA and 40/60 SBR/EVA blends are presented in Fig. 10. It is interesting to note that T_g of the phases are shifted to the higher temperature region in peroxide cured blend
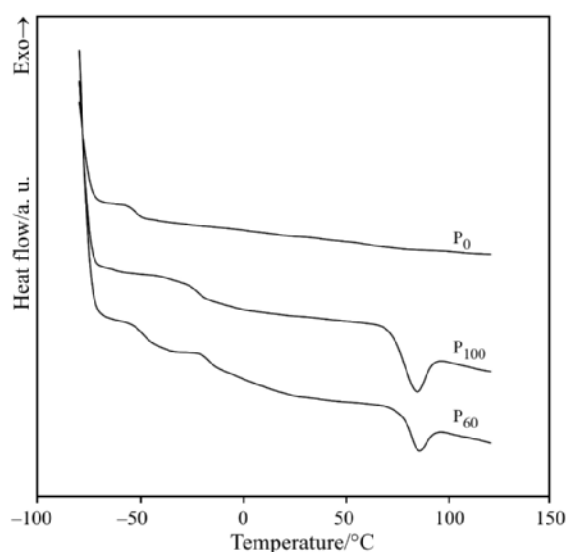
components and 40/60 SBR/EVA blend. This is due to the restriction on the segmental motion of the polymeric chains due to cross-linking. The melting temperature (T_m), heat of fusion (ΔH), fractional crystallinity (X_C) and glass transition (T_g) of the peroxide cured blends are reported in Table 6.

DSC traces of the 40/60 SBR/EVA blends with different cross-linking systems are compared in Fig. 11. It is interesting to note that in the case of cross-linked systems depending on the type of cross-linking agent used, the T_gs of the SBR and EVA phases undergo substantial shift from their normal positions to higher tem-

Table 6 Crystallisation characteristics of EVA phase in uncross-linked, cross-linked and compatibilized SBR/EVA systems

Sample	SBR/%	EVA/%	ΔH/J mol^{-1}		Crystallinity (X_C)/%		T_m/°C	T_g (SBR)/°C	T_g (EVA)/°C
			a	b	c	d			
SBR	100	–	–	–	–	–	–	−56.7	–
40/60 SBR/EVA	40	60	25.32	24.5	19.2	18.58	84.8	−51.7	−24.2
EVA	–	100	42.20	41.7	32.0	31.62	85.9	–	−25.9
P_0	100	–	–	–	–	–	–	−52.5	–
P_{20}	80	20	8.44	7.9	6.4	5.99	84.7	−51.7	–
P_{40}	60	40	16.88	15.4	12.8	11.68	83.4	−46.8	−19.3
P_{60}	40	60	25.32	23.7	19.2	17.97	82.5	−45.3	−18.5
P_{80}	20	80	33.76	32.2	25.6	24.42	83.8	−46.1	−18.7
P_{100}	–	100	42.20	40.6	32.0	30.78	–	–	−21.6
S_{60}	40	60	25.32	24.1	19.2	18.27	84.9	−47.5	−23.2
M_{60}	40	60	25.32	23.6	19.2	17.91	82.8	−47.1	−22.3
$P_{60}C_6$	40	60	25.32	23.2	19.2	17.52	83.6	−44.6	−17.1
$S_{60}C_6$	40	60	25.32	23.8	19.2	18.02	85.3	−46.4	−22.5

a – theoretical – ΔH calculated by the expression – 42.2·[EVA]/100; b – experimental – ΔH determined from the area of the melting endotherm; c – theoretical – fractional crystallinity calculated from the ΔH values, assuming that 42.2 J mol^{-1} corresponds to 32% of crystallinity of EVA18; d – experimental – crystallinity determined from the experimental values of ΔH
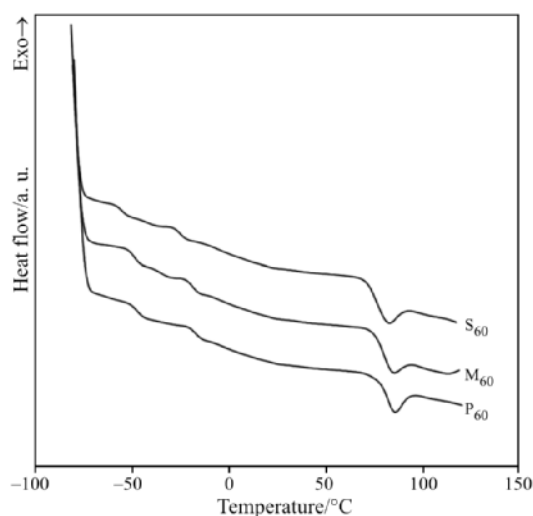
Fig. 11 DSC curves of 40/60 SBR/EVA blend with different cross-linking systems
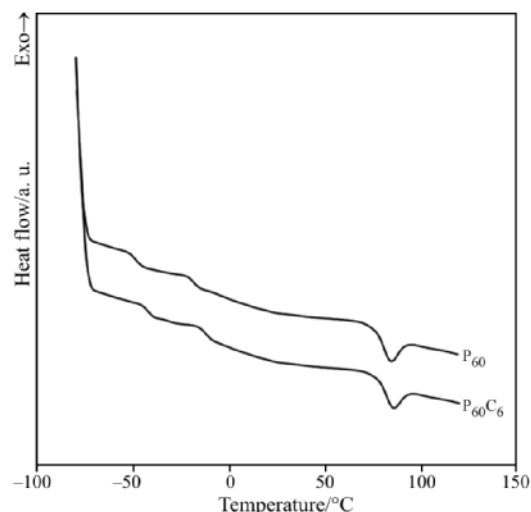

Fig. 12 DSC curves of peroxide cured uncompatibilized and compatibilized 40/60 SBR/EVA blends

perature regions. Generally the introduction of cross-links increases the T_g value due to the restriction on the segmental motion of the polymeric chain by the cross-linking. When sulphur is used as the cross-linking system the SBR phase is preferentially cross-linked, where as DCP cross-links both the phases. In mixed system, sulphur preferentially cross-links the SBR phase and DCP cross-links both the phases. In 40/60 SBR/EVA blends, the T_g of SBR and EVA phases for sulphur, peroxide and mixed systems are (–47.5 and –23.2°C), (–45.3 and –18.5°C) and (–47.1 and –22.3°C) respectively. The T_gs of SBR and EVA phases in the un-cross-linked 40/60 SBR/EVA blend are –51.7 and –24.2°C, respectively. From these results it can be concluded that increase in T_g of SBR and EVA phase with the introduction of cross-links is maximum, when DCP is used as the cross-linking system.

DSC results of the 40/60 peroxide cured SBR/EVA blends with 6 phr compatibilizer are given in Fig. 12 and in Table 6. The glass transition temperature is shifted towards the higher temperature region upon compatibilization. This could be due to the enhanced interfacial adhesion between the blend components provided by the compatibilizer. The degree of crystallinity of uncross-linked blends is close to the theoretical value. However, for cross-linked and compatibilized systems, there is a decrease in the overall crystallinity which can be attributed to the increased interaction between the blend components which subsequently inhibits the crystal growth in the EVA phase.

Conclusions

The thermal behaviour of SBR/EVA blends was studied using TG and DSC, with respect to the blend composition, cross-linking systems and a compatibilizer. TG showed that blends are thermally more stable than the individual components. The initial decomposition temperature (T_0) and 50% decomposition (T_{50}) increased with EVA content. This is due to the enhanced interfacial adhesion between the blend components. It was found that mass loss of the blend at any temperature was lower than that of the homopolymers. This showed that blending improved the overall thermal behaviour of the components. The peroxide cured system exhibited the highest initial decomposition temperature indicating its better thermal stability. The blends exhibited higher activation energy than the components, which was further increased upon compatibilization. DSC studies revealed that even by the addition of the compatibilizer, SBR/EVA system is thermodynamically immiscible. This is evident from the presence of two different glass transition temperatures, corresponding to SBR and EVA phases in the compatibilized and uncompatibilized system.

References

1 I. C. McNeill, Thermal Degradation, in Comprehensive Polymer Science, Vol. 6, G. Allen, Ed., Pergamon Press, New York 1989, Ch. 15.
2 S. H. El-Sabbah, Polym. Test., 22 (2003) 93.
3 M. T. Ramesan, G. Mathew, B. Kuriakose and R. Alex, Eur. Polym. J., 37 (2001) 719.
4 O. Slisenko, E. Lebedev, P. Pissis, A. Spanoudaki, E. Kontou and O. Grigoryeva, J. Therm. Anal. Cal., 84 (2006) 15.
5 P. Rybiński, G. Janowska, W. Antkowicz and S. Krauze, J. Therm. Anal. Cal., 81 (2005) 9.
6 K. Pielichowski and A. Leszczyńska, J. Therm. Anal. Cal., 78 (2004) 631.

7 S. V. Natasa and K. Ivka, Polym. Degrad. Stab.,
   84 (2004) 23.

8 P. Thavamani and D. Khastgir, J. Elastomers Plast.,
   29 (1997) 124.

9 V. Schmidt, S. C. Domenech, M. S. Soldi, E. A. Pinheiro
   and V. Soldi, Polym. Degrad. Stab., 83 (2004) 519.

10 I. A. Amraee, A. A. Kathab and S. A. Jollah,
   Rubber Chem. Technol., 69 (1995) 130.

11 S. Ahmed, A. A. Basfar and M. M. Abdel Aziz,
   Polym. Degrad. Stab., 67 (2002) 319.

12 M. De Sarkar, P. G. Mukunda, P. De Prajna and
   A. K. Bhowmick, Rubber Chem. Technol., 70 (1997) 855.

13 P. Ghosh, B. Chattopadhyay and K. Achintya, Eur. Polym. J.,
   32 (1996) 1015.

14 A. M. Rocco, C. E. Bielschowsky and R. P. Pereira,
   Polymer, 44 (2003) 361.

15 M. Lai and J. Liu, J. Therm. Anal. Cal., 77 (2004) 935.

16 C. K. Radhakrishnan, A. Sujith, G. Unnikrishnan and
   S. Thomas, J. Appl. Polym. Sci., 94 (2004) 827.

17 C. K. Radhakrishnan, B. Ganesh, A. Sujith, G. Unnikrishnan
   and S. Thomas, Polym. Polym. Compos., 13 (2005) 335.

18 C. K. Radhakrishnan, R. Alex and G. Unnikrishnan,
   Polym. Degrad. Stab., 91 (2006) 902.

19 N. Grassie, Encyl. Polym. Sci. Tech., Wiley, New York,
   Vol. 4 (1967) 159.

20 A. T. Koshy, B. Kuriakose, S. Thomas and S. Varghese,
   Polymer, 71 (1992) 3428.

21 E. Martuscelli, Polym. Eng. Sci., 24 (1984) 563.